PAPER

Check for updates

A multi-loop aptamer-based fluorescent aptasensor for enhanced detection of 17β-estradiol†

Pakawat Kongpreecha,[a] Arnon Buntha,[a] Pattama Tongdee,[bc] Pinwen Peter Chiou[d] and Sineenat Siri [ID] *[a]

The modulation of 17β-estradiol (E2) level, even in trace amounts outside the normal range, plays a critical role in diagnosing and treating various diseases in females. This work presents a novel, simple, and highly sensitive method for E2 detection based on the designed repetitive-loop aptamer. The method is based on the different fluorescence intensities of SYBR Green I (SGI) to intercalate the DNA aptamer structures, which are changed upon interacting with E2. Among the designed aptamers containing 1–5 loop structures (designated as O1–O5), the O5-aptamer exhibited the highest E2 interaction and was employed to construct the O5-aptasensor. Under optimal conditions, the aptasensor displayed excellent sensitivity, with a linear detection range of 1–200 pM, a limit of detection (LOD) of 1.34 pM, and a limit of quantification (LOQ) of 4.48 pM. Its LOD is 13.5 folds lower than that of the L1-aptasensor. The O5-aptasensor specifically detected E2, distinguishing it from structurally similar compounds such as progesterone, genistein, diethylstilbestrol, bisphenol A, and chloramphenicol. Furthermore, the O5-aptasensor accurately detects E2 spiked in artificial urine and human serum samples, with recovery rates ranging from 98.73% to 109.00%, and relative standard deviations below 8%. The O5-aptasensor was tested on blood serum samples from seven hospital patients, and its performance was comparable to that of the hospital analysis for E2 measurement. These findings highlight the potential of the O5-aptasensor as a highly sensitive platform for clinical E2 detection, offering a viable alternative to existing methods.

1. Introduction

17β-Estradiol (E2) is a crucial endogenous estrogen primarily synthesized in the ovaries and plays a key role in regulating the development of female secondary sexual characteristics.[1] Typically, E2 levels in reproductive women are within the range of 50 to 300 pg ml^{-1} (about 184 to 1101 pM), while in postmenopausal women, the levels drop to below 10 pg ml^{-1} (about 37 pM).[2] However, low E2 levels, different from its normal range, are associated with the occurrence of polycystic ovary syndrome, osteoporosis, abdominal aortic aneurysms, turner syndrome, and hypogonadism in women.[3] Therefore, an accurate and sensitive E2 detection method is essential to monitor E2 levels for diagnosing and treating related diseases. Classically, liquid chromatography-mass spectrometry (LC-MS)[4] and high performance liquid chromatography (HPLC)[5] have been commonly used to detect E2 in laboratory samples. Although these methods offer high accuracy and sensitivity, they are costly, time-consuming, intricate, and necessitate skilled personnel. Consequently, the need for an uncomplicated, affordable, and user-friendly E2 detection method is increasing.

In the past few years, there has been a significant rise in adopting biosensors for E2 detection, driven by their simplicity, cost-effectiveness, and rapid analytical techniques. Aptamer-based biosensors, commonly referred to as aptasensors, have gained considerable prominence as detection systems for specific targets like small molecules, proteins, or even entire cells.[6] This approach provides several advantages, including cost-effective manufacturing, high selectivity, and convenient preparation capabilities.[7] Aptamers are short single-stranded oligonucleotides that possess a unique characteristic of folding into specific structures,[8] enabling them to bind to various targets through hydrogen bonding, electrostatic interactions, and hydrophobic forces.[9] Through the integration of aptamers with various transducers, various types of aptasensors have been established, such as luminescence aptasensors,[10]

[a]School of Biology, Institute of Science, Suranaree University of Technology, Nakhon Ratchasima 30000, Thailand. E-mail: ssinee@sut.ac.th

[b]School of Obstetrics and Gynecology, Institute of Medicine, Suranaree University of Technology, Nakhon Ratchasima, Thailand

[c]Suranaree University of Technology Hospital, Suranaree University of Technology, Nakhon Ratchasima, Thailand

[d]Department of Aquaculture, National Taiwan Ocean University, Keelung, Taiwan

† Electronic supplementary information (ESI) available. See DOI: https://doi.org/10.1039/d5ay00154d

colorimetric aptasensors,[11] fluorescence aptasensors,[12] and electrochemical aptasensors.[13] Among these aptasensors, fluorescent aptasensors have gained attraction to develop an efficient E2 detection method due to their high sensitivity, wide linear range, fast response time, and simplicity in operation.[14] With these advantages, many studies reported the development of fluorescent aptasensors to detect E2. For example, Huang and colleagues designed a fluorescent aptasensor that includes a Ru complex, a quantum dot, and an aptamer. The binding between E2 and the aptamer facilitates the association of the positively charged ruthenium complex with the negatively charged quantum dot. This interaction results in a reduction in the fluorescence intensity of the quantum dot. The LOD achieved by this technique is 37 nM.[15] Next, a fluorescence aptasensor, developed by Zhang and colleagues, employed a FAM-labeled aptamer and a BHQ-labeled partially complementary sequence. When E2 is present, the aptamer dissociates from the duplex structure, leading to a notable enhancement in fluorescence intensity. Utilizing this aptasensor, E2 detection achieves an LOD of 0.35 nM.[16] Later, a novel fluorescence aptasensor was developed by linking the E2 aptamer to carbon quantum dots and connecting its complementary DNA sequence with magnetic nanoparticles. Without E2, the E2 aptamer forms a hybrid with complementary DNA, which can be separated by a magnet. As a result, the E2 aptamer-carbon quantum dot complex is not present in the solution, leading to a low fluorescence intensity. However, in the presence of E2, the aptamer is released from hybridization and binds to E2. Even after magnetic separation, the E2 aptamer-carbon quantum dot complex remains in the solution, resulting in a high fluorescence intensity. This system exhibits highly sensitive detection of E2, with an LOD as low as 3.48 pM.[17] Although this aptasensor demonstrated remarkable E2 detection capability, its usage entailed a complex procedure. Consequently, developing a simple fluorescent aptasensor with high measurement efficiency is a research challenge.

The utilization of DNA staining dyes in label-free fluorescent aptasensors has attracted interest due to their simplicity, cost-effectiveness, ease of application, and independence from specialized expertise.[14] Among these dyes, SYBR Green I (SGI), a selective intercalating dye, is commonly employed in label-free fluorescence detection methods. It offers low toxicity, remarkable stability, and the ability to bind to single-stranded DNA, including aptamers, resulting in robust fluorescence emission.[18] Drawing on its advantageous features, SGI has been successfully utilized alongside aptamers for detecting diverse targets such as tobramycin,[14] clenbuterol,[19] and testosterone.[20] Previous studies have demonstrated the potential of SGI (SYBR Green I) and aptamers in the detection of E2. SGI is known to intercalate within the aptamer structure, absorbing excitation light and subsequently emitting fluorescence. Upon the introduction of E2 into the system, the aptamers exhibit selective binding to E2 molecules, resulting in the displacement of SGI and a corresponding decrease in fluorescence intensity. This mechanism has been utilized for E2 detection with a reported limit of detection (LOD) of 2.4 nM.[21] In this work, we utilized aptamers containing 1–5 internal loops to develop a fluorescence-based aptasensor leveraging the multiloop aptamer structure in conjunction with SGI. The multiloop design is anticipated to enhance the binding efficiency and fluorescence signal transduction, enabling highly sensitive E2 detection. This novel approach builds on the established benefits of SGI and multiloop aptamer systems, aiming to further improve detection performance and broaden the application of label-free fluorescent aptasensors in clinical diagnostics.

2. Experimental section

2.1 Materials and reagents

All oligonucleotides in this experiment were obtained from Bio Basic Asia Pacific Pte Ltd (Singapore City, Singapore). SYBR Green I (SGI) was bought from AppliChem (Darmstadt, Germany). Disodium hydrogen phosphate and potassium chloride were purchased from BDH Inc. (Toronto, Canada). Potassium dihydrogen phosphate and ammonium hydroxide were bought from Merck Millipore (Darmstadt, Germany). Tris–HCl buffer was brought from Vivantis (Selangor Darul Ehsan, Malaysia). Magnesium sulfate, chloramphenicol, genistein, diethylstilbestrol, bisphenol A, 17β-estradiol (E2), 3-(N-morpholino)-propanesulfonic acid (MOPS), and human serum from human male AB plasma, USA origin, sterile-filtered were purchased from Sigma-Aldrich (St Louis, MO, USA). Progesterone was purchased from Tokyo Chemical Industry (Tokyo, Japan). Urea was purchased from QRec (Auckland, New Zealand). Sodium chloride (NaCl), potassium chloride (KCl), and calcium chloride (CaCl$_2$) were bought from BDH (Poole, English).

2.2 E2–aptamer binding efficiency

The designed aptamers (O1–O5, Fig. 1) were evaluated for their binding to E2. Aptamers were denatured at 95 °C for 5 min and subsequently cooled at 25 °C for 10 min. In a total reaction of 200 μl, each aptamer (400 nM) was incubated with E2 (450 μM) for 30 min before the addition of SGI (0.8×). After incubation for 20 min, the fluorescence intensity of the mixture was measured using a microplate reader (BMG Labtech, Ortenberg, Germany) with excitation at 497 nm and emission at 520 nm. In the control, E2 was substituted with DI water. The efficiency of each aptamer was determined using eqn (1), where F_0 and F represent the fluorescence intensities of reactions without and with E2, respectively.
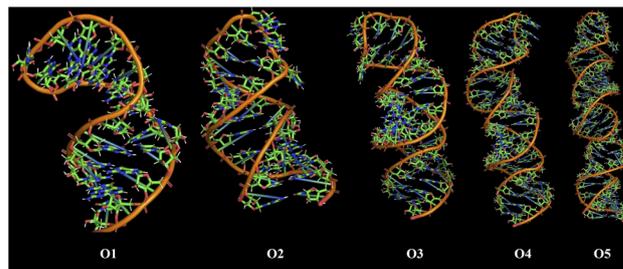

Fig. 1 Aptamers O1, O2, O3, O4, and O5.

$$\text{DNA aptamer binding efficiency} = F_0 - F \quad (1)$$

2.3 Development of E2-aptasensor

The development of the E2-aptasensor involved optimizing various conditions, including the type of buffer, pH, SGI concentration, aptamer concentration, E2–aptamer incubation time, and SGI incubation time. Each optimization step is detailed below.

To evaluate the most suitable buffer type, a reaction mixture containing 200 nM aptamer and 450 μM E2 was prepared and incubated at 25 °C for 40 min in one of the following buffers: MOPS, Tris–HCl, phosphate-buffered saline (PBS), or Milli-Q water, with a total reaction volume of 200 μl. Subsequently, SGI (0.2×) was added to the reaction mixture, followed by an additional incubation for 20 min. Fluorescence intensity was measured using a microplate reader with an excitation wavelength of 497 nm and an emission wavelength of 520 nm. A reaction without E2 served as the negative control. The optimal buffer type was determined based on the maximum difference (ΔF) between fluorescence intensities F_0 (negative control) and F (reaction with E2).

For pH optimization, the selected buffer's pH was adjusted within the range of 5–9 using HCl or NaOH. The buffer was then used to incubate 200 nM aptamer and 450 μM E2 at 25 °C for 40 min. Afterward, SGI (0.2×) was added, followed by a 20 min incubation. Fluorescence intensity was measured under the same conditions as before. The optimal pH was identified as the value yielding the highest ΔF.

To determine the optimal SGI concentration, a reaction mixture containing 200 nM aptamer and 450 μM E2 was incubated at 25 °C for 40 min in the selected buffer at the optimized pH. SGI was added at concentrations of 0×, 0.1×, 0.2×, 0.4×, 0.8×, and 1.6×, followed by a 20 min incubation. Fluorescence intensity was measured, and a reaction without E2 was used as the negative control. The optimal SGI concentration was defined as the concentration that provided the maximum ΔF.

For the optimal aptamer concentration, various aptamer concentrations (0, 25, 50, 100, 200, 400, 600, and 800 nM) were incubated with 450 μM E2 at 25 °C for 40 min in the selected buffer at the optimized pH. SGI was then added at its optimized concentration, followed by a 20 min incubation. Fluorescence intensity was measured, with a reaction without E2 serving as the negative control. The optimal aptamer concentration was determined as the concentration that yielded the maximum ΔF.

To optimize the incubation time between E2 and the aptamer, 450 μM E2 and the aptamer at its optimized concentration were incubated for varying durations (10, 20, 30, 40, 50, and 60 min) at 25 °C in the selected buffer at the optimized pH. After incubation, SGI (optimized concentration) was added and incubated for 20 min. Fluorescence intensities were measured, and the optimal E2–aptamer incubation time was identified as the duration that provided the highest ΔF.

The incubation time of SGI was optimized by first incubating the aptamer (optimized concentration) and 450 μM E2 at the optimized time and under optimized conditions. SGI (optimized concentration) was then added and incubated for 5, 10, 15, 20, 25, and 30 min. Fluorescence intensity was measured, and the ΔF was calculated for each incubation time. The optimal SGI incubation time was determined as the duration yielding the highest ΔF.

2.4 Sensitivity of detection

The reactions were carried out by incubating the aptamer (optimal concentration) with E2 (1–2000 pM) for 30 min. Then, SGI (0.8×) was added and incubated for 20 min. Then, the fluorescence intensity was measured with excitation at 497 nm and emission at 520 nm to determine the F and F_0 values. The limit of detection (LOD) was calculated using eqn (2) and the limit of quantification (LOQ) was calculated *via* eqn (3), where σ is the standard deviation of the blank solution and S is the slope of the calibration curve.

$$\text{LOD} = 3\sigma/S \quad (2)$$

$$\text{LOQ} = 10\sigma/S \quad (3)$$

2.5 Selectivity of detection

The selectivity of the developed aptasensor was evaluated using 17β-estradiol (E2), diethylstilbestrol (DES), progesterone (P4), genistein (GEN), bisphenol A (BPA), and chloramphenicol (CPL) as test analytes. Each chemical, at a concentration of 160 pM, was incubated with the aptamer for 30 min under optimized conditions. Subsequently, SYBR Green I (SGI) was added, and the mixture was further incubated for 20 min to facilitate fluorescence development. The fluorescence intensity of each sample was measured and compared to the fluorescence intensity obtained with E2 to assess the aptasensor's selectivity.

2.6 E2-spiked test

Artificial urine was prepared following the protocol described by Galay *et al.*[22] Standard E2 was spiked into artificial urine and human serum at final concentrations of 2, 20, 40, and 80 pM. The aptasensor was tested with these E2-spiked samples by incubating the aptamer with each sample for 30 min, followed by adding SGI. After an additional 20 min incubation, the fluorescence intensity was measured. The E2 concentration in spiked samples was calculated using a standard curve generated by plotting the fluorescence change ($F_0 - F$) against known E2 concentrations. The percent recovery of E2 was determined by eqn (4), where C_{detected} is the detected E2 concentration by the developed aptasensor, and C_{added} is the actual concentration of the spiked E2. The relative standard deviation (RSD) was calculated using eqn (5), where S stands for the standard deviation and $\bar{x}$ is the sample mean.

$$\text{Recovery rate} = (C_{\text{detected}}/C_{\text{added}}) \times 100\% \quad (4)$$

$$\text{Relative standard deviation} = (S/\bar{x}) \times 100\% \quad (5)$$

2.7 Determination of E2 in volunteers' blood

This study was approved by the Ethics Committee of Suranaree University of Technology (Ethics Authorization Code EC-65-92) and conducted in compliance with institutional guidelines, relevant regulations, and the principles of the Declaration of Helsinki. Blood samples were obtained from voluntary donors at Suranaree University of Technology Hospital after obtaining written informed consent. Sample collection was performed by certified medical laboratory technologists using sterile venipuncture, and the blood was collected in additive-free tubes. The samples were then centrifuged at $1000 \times g$ for 10 min at 25 °C to separate the serum. The resulting serum was aliquoted and stored at −80 °C until analysis. The developed aptasensor was evaluated using these blood serum samples. Each serum sample was incubated with the aptamer for 30 min, followed by the addition of SGI. After an additional 20 min incubation, the mixture was diluted 10-fold before fluorescence intensity measurement. The concentration of E2 in the serum was calculated using a standard curve, and the results were compared with hospital-measured values to assess the accuracy of the aptasensor.

2.8 Statistical analysis

For all analyses at least five replicates were performed to determine the average and standard deviation. The statistical analysis was performed using SPSS 11.5 (Chicago, IL, USA). One-way ANOVA was used to analyze the variance of more than 2 sample groups, and Tukey's honestly significant difference test was carried out to compare the differences between all pairs of observations. The statistical difference is significant at $P < 0.05$.

3. Results and discussion

3.1 Binding capability of multiple loop aptamers to E2

The binding capabilities of five aptamers (O1–5) containing 1–5 loop structures were evaluated for their interaction with E2 using the SGI competitive binding assay. As shown in Fig. 2, all tested aptamers demonstrated binding to E2, with binding efficiency increasing proportionately to the number of loop structures. This
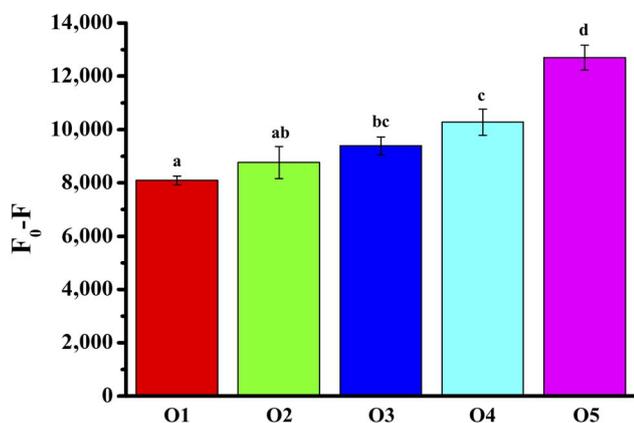
Fig. 2 The binding capability of the designed aptamers.

trend is evident from the progressively higher $F_0 - F$ values observed with the aptamer containing more loop regions. Among the tested aptamers, O5 exhibited the highest binding capability, likely due to its greater number of E2-binding sites. This enhanced binding efficiency aligns with previous studies that suggest multi-loop aptamers provide improved target interaction through increased binding site availability.[23] Consequently, the O5-aptamer was selected for further development as a fluorescence-based aptasensor for E2 detection.

3.2 Development of the fluorescent aptasensor

The developed aptasensor operates based on the intercalation of SGI into the three-dimensional structure of the aptamer, as illustrated in Fig. 3. In the absence of E2, SGI intercalates into the aptamer structure, emitting a strong fluorescence signal. Conversely, in the presence of E2, the aptamer prefers binding to E2, leading to the formation of a stable complex structure. Subsequently, lesser SGI can access and intercalate into the structure of the aptamer, causing a decline in fluorescence signal.[18] Therefore, the change in fluorescence intensity can be employed to analyse the presence of E2 in the sample quantitatively.

The feasibility of this proposed aptasensor was tested by examining the changes in SGI fluorescence intensity under various conditions, as seen in Fig. 4. SGI alone and SGI combined with E2 exhibited very low fluorescence intensity, confirming that SGI fluoresces minimally in the absence of DNA and that E2 does not directly affect SGI fluorescence. When SGI was combined with the aptamer, a significant increase in fluorescence intensity was observed, indicating successful intercalation of SGI into the aptamer's structure. In contrast, when the aptamer, E2, and SGI were combined, a notable decrease in fluorescence intensity occurred. This reduction is attributed to the specific binding between the aptamer and E2, which impedes SGI from intercalating into the aptamer's structure, thereby reducing fluorescence.[18] These results validate the proposed mechanism of the E2 aptasensor, demonstrating its potential for sensitive and specific detection of E2 based on the fluorescence changes observed.

3.3 Optimization of detection conditions

To optimize the detection conditions for the aptasensor, several parameters, including buffer composition, pH, SGI
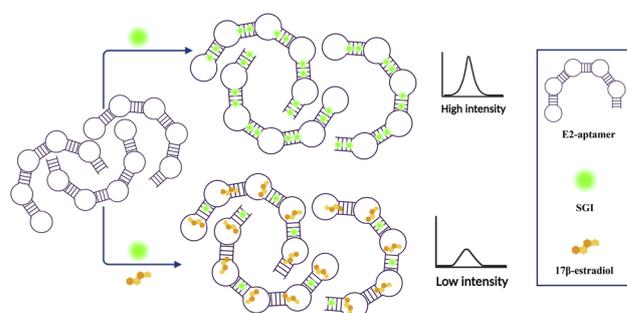
Fig. 3 The schematic model of the developed aptasensor to detect E2.
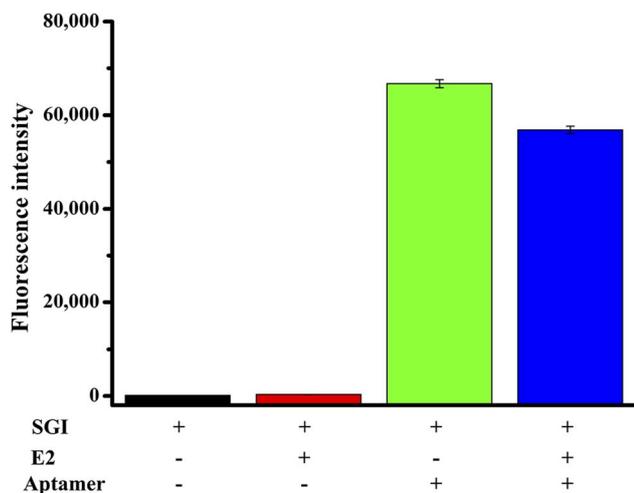
Fig. 4 The feasibility test of the developed aptasensor as determined by the fluorescence spectra of SGI under various conditions.

concentration, aptamer concentration, and incubation times, were systematically investigated.

The influence of buffer composition was examined using MOPS, Tris–HCl, and PBS, compared to Milli-Q water. As shown in Fig. 5(A), the MOPS buffer exhibited the highest fluorescence difference ($F_0 - F$), significantly outperforming the other buffers. This result suggests that buffer composition strongly impacts the interaction between the aptamer and SGI, likely due to the buffering range and capacity provided by MOPS. MOPS buffer appears to create a favorable microenvironment for protonation and

deprotonation processes, thereby enhancing the fluorescence intensity.[24] The optimal pH for MOPS buffer was determined by testing pH values ranging from 5 to 9. Fig. 5(B) shows that the highest $F_0 - F$ value was observed at pH 7. This pH likely supports the most effective interaction between the aptamer and SGI, facilitating maximal fluorescence intensity.

The SGI concentration was optimized by testing concentrations ranging from $0.1\times$ to $1.6\times$. Fig. 5(C) indicates that the optimal SGI concentration was $0.8\times$, which yielded the highest $F_0 - F$ value. A lower SGI concentration may be insufficient for accurate fluorescence measurement, while an excessively high concentration could interfere with aptamer–E2 binding.

Aptamer concentrations ranging from 25 to 800 nM were evaluated. The results, shown in Fig. 5(D), indicate that the optimal concentration was 400 nM, the lowest concentration that achieved the highest $F_0 - F$ value. Insufficient aptamer concentrations may reduce detection sensitivity, while excessive concentrations could disrupt accurate fluorescence-based measurement.

The incubation time for the aptamer–E2 interaction varied from 10 to 60 min. Fig. 5(E) reveals that the optimal incubation time was 30 min, which provided the shortest duration while achieving the highest $F_0 - F$ value.

The optimal incubation time for SGI intercalation was investigated by varying the time from 5 to 30 min. As illustrated in Fig. 5(F), the highest $F_0 - F$ value was achieved at 20 min, making it the optimal SGI incubation time.

3.4 Sensitivity of detection

The sensitivity of E2 detection using the developed aptasensors was evaluated with standard E2 concentrations ranging from 0 to 2000 pM. For this study, two aptasensors were constructed: the O1-aptasensor (using the single-loop O1 aptamer) and the O5-aptasensor (using the multi-loop O5 aptamer). As depicted in Fig. 6(A) and (B), both aptasensors demonstrated a linear detection range of 1–200 pM for E2. The limit of detection (LOD) and limit of quantification (LOQ) were determined for each aptasensor. The LOD and LOQ of the O1-aptasensor were 20.54 pM and 62.25 pM, respectively. In contrast, the O5-aptasensor exhibited significantly improved sensitivity, with an LOD of 1.34 pM and an LOQ of 4.48 pM. Notably, the LOD of the O5-aptasensor was 15.3 times lower than that of the O1-aptasensor, indicating that the multiple loop aptamer provides superior binding efficiency and detection sensitivity compared to the single-loop aptamer. The enhanced sensitivity of the O5-aptasensor, coupled with its broad linear detection range, suggests its potential for accurately detecting low E2 concentrations, such as those typically observed in post-menopausal women, where E2 levels are often below 36.71 pM.[2] This capability is particularly valuable for aiding in the diagnosis of related symptoms. Furthermore, a comparison with other reported E2 detection systems, summarized in Table 1, highlights the superior sensitivity of the developed O5-aptasensor. This improved performance underscores its potential as a reliable and effective tool for E2 detection in clinical and diagnostic applications.
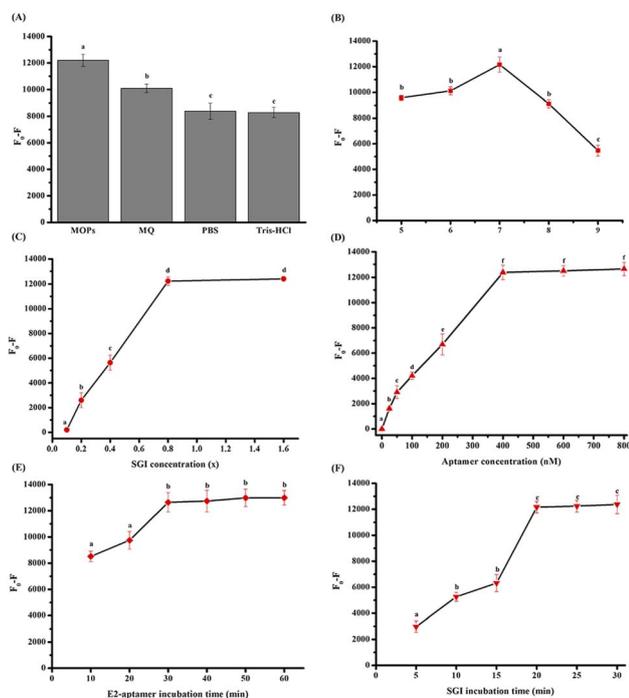

Fig. 5 Optimal conditions for the aptasensor; (A) types of buffers, (B) pH, (C) SGI concentration, (D) aptamer concentration, (E) aptamer–E2 incubation time, and (F) SGI incubation time.
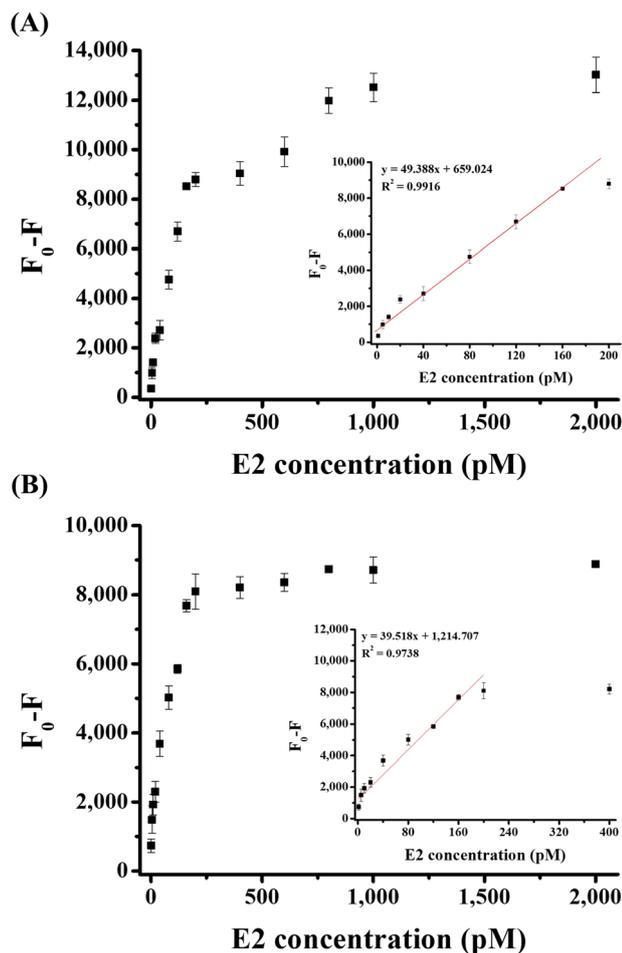
(A)

(B)

Fig. 6 Sensitivity of E2 detection by (A) O5-aptasensor and (B) O1-aptasensor.

3.5 Selectivity of detection

The selectivity of the O5-aptasensor was evaluated by testing it against various structurally similar chemicals, including chloramphenicol (CPL), diethylstilbestrol (DES), bisphenol A (BPA), progesterone (P4), and genistein (GEN). Additionally, the aptasensor's response to a mixture of E2 and all tested compounds (MIX) was evaluated. The results, illustrated in Fig. 7, demonstrate that the developed aptasensor specifically binds to E2, with negligible interaction with the other tested compounds. This high selectivity can be attributed to the critical nucleotides in the aptamer sequence, particularly within the multiple-loop structure of the O5 aptamer. These nucleotides enable precise molecular recognition and binding to E2, ensuring minimal cross-reactivity with structurally similar substances.[23] A previous computational simulation study suggested that the specificity of the O5 aptamer for E2 arises from key molecular interactions, including hydrogen bonding between cytosine and the hydroxyl group at the 3-position of E2, hydrogen bonding between thymine and the hydroxyl group at the 17β-position, and π-stacking interactions between thymine and the A-ring of E2.[35] Although other tested compounds share structural similarities with E2, variations in their functional groups and
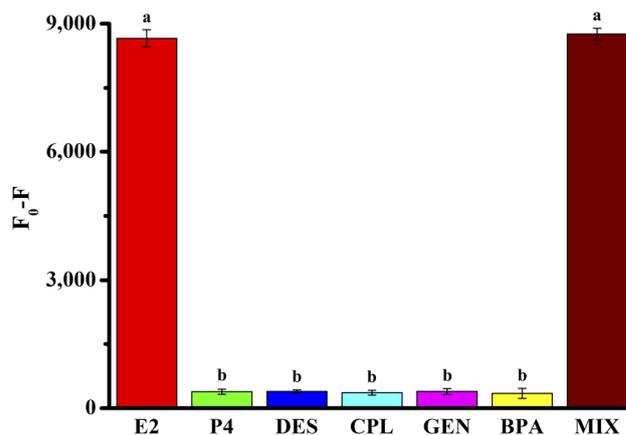

Fig. 7 The detection selectivity of the aptasensor.

hydroxyl positioning lead to only weak binding interactions with the O5-aptasensor. These findings confirm the robustness and specificity of the O5-aptasensor for detecting E2. Its exceptional selectivity makes it a promising tool for applications requiring precise E2 measurement without interference from other compounds with comparable structures.

3.6 Stability of the aptasensor

The stability of the O5-aptasensor for detecting E2 was evaluated over a 7 day period. The component suspensions of the aptasensor system were stored at 4 °C and used for E2 detection daily. As shown in Fig. 8, the O5-aptasensor remained capable of detecting E2, with only a slight decrease in fluorescence intensity that was not statistically significant. This reduction is likely due to the gradual degradation of the aptamer or the decrease in fluorescence of the SGI solution at 4 °C, as suggested by the manufacturers. In our opinion, since the O5-aptasensor comprises an aptamer, SGI, and standard E2, its components in aqueous form may degrade over time when stored at 4 °C. To ensure long-term stability, an aptamer should be aliquoted, stored in solid form and reconstituted prior to use, while SGI should be kept at −20 °C prior to use.
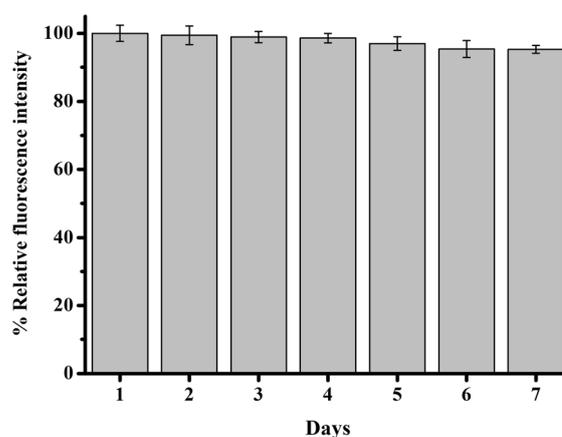

Fig. 8 The storage stability evaluation of the aptasensor over a 7 day period.

Table 1 Comparison between the developed aptasensor and the reported E2 sensors

Detection method	LOD (pM)	References
Pt/Se electrochemical sensor	11 120	25
Digital immunoassay	3.67	26
Liquid chromatography-tandem mass spectrometry	29.37	27
Colorimetric aptasensor	13.1	23
Ratiometric self-powered aptasensor	120	28
Molecularly imprinted ratiometric fluorescent sensor	12.12	29
CDs@MI-PDA fluorescence sensor	1248.26	30
Ratiometric fluorescence aptasensor	200	31
Electrochemical aptasensor	3	32
Fluorescence aptasensor	56	33
Fluorescence aptasensor	9703.36	34
Fluorescence aptasensor	1.34	This work

Table 2 E2 detection by the O5-aptasensor in E2-spiked artificial urine and human serum samples ($n = 5$)

Samples	Spiked E2 (pM)	Detected E2 (pM)	Recovery (%)	RSD (%)
Artificial urine	2	2.09 ± 0.16	104.50	7.66
	20	20.82 ± 1.24	104.10	5.96
	40	39.49 ± 1.80	98.73	4.56
	80	84.46 ± 5.38	105.58	6.37
Human serum	2	2.18 ± 0.13	109.00	5.96
	20	19.89 ± 1.57	99.45	7.89
	40	42.18 ± 2.45	105.45	5.81
	80	80.02 ± 4.15	100.03	5.19

3.7 E2-spiked test in artificial urine and human serum samples

The performance of the O5-aptasensor in detecting E2 in artificial urine and human serum samples was assessed by spiking known concentrations of E2 (2, 20, 40, and 80 pM) into these matrices. In artificial urine, the recovery rates for E2 ranged from 98.73% to 105.58%, with relative standard deviation (RSD) values between 4.56% and 7.66%. In human serum, the E2 recovery rates were between 99.45% and 109.00%, with RSD values consistently below 8% (Table 2). These recovery rates fall within the acceptable range of 70–120%, and the RSD values are well within the precision criterion of ≤15%,[36] indicating the high accuracy and reliability of the aptasensor. The results demonstrate that the O5-aptasensor performs exceptionally well in detecting E2 in complex biological fluids, making it a promising tool for accurate and reliable E2 measurement in clinical and diagnostic applications.

3.8 Precision test compared with hospital analysis results

The O5-aptasensor was employed to measure E2 levels in blood samples from seven patient volunteers (S1–S7) at Suranaree University of Technology Hospital. The results obtained with the aptasensor were compared with those from the hospital's standard analysis method, with each analysis conducted in triplicate. As shown in Table 3, the precision of the aptasensor ranged from 88.91% to 102.10% when compared to the hospital analysis results. These findings suggest that the O5-aptasensor offers reliable precision for E2 detection in blood samples, supporting its potential use in clinical settings. However, testing with additional blood samples is recommended to further validate its accuracy and robustness.

4. Conclusions

This study presents a simple, highly sensitive fluorescence aptasensor for E2 detection, utilizing a repetitive loop structure aptamer specific to E2 combined with a fluorescent dye. The binding assay revealed that the O5 aptamer, with its five-loop structure, exhibited the highest binding affinity to E2 compared to the L1–L4 aptamers, which contain 1–4 loops, respectively. Consequently, the O5-aptasensor was developed and evaluated for its ability to detect E2 based on the differential fluorescence intensity of SGI under E2–aptamer binding and aptamer-alone conditions. Under optimized conditions,

Table 3 Comparison of E2 measurement by the developed aptasensor and the hospital analysis results in human blood serum

Blood serum samples	E2 concentration (pM)		Precision (%)
	Aptasensor	Hospital analysis	
S1	51.02 ± 0.76	50.94	100.16
S2	126.31 ± 12.12	142.07	88.91
S3	511.94 ± 4.40	524.37	97.63
S4	129.26 ± 2.04	137.48	94.02
S5	40.62 ± 2.09	42.61	95.33
S6	132.43 ± 3.97	129.70	102.10
S7	60.34 ± 1.86	64.15	94.06

the O5-aptasensor demonstrated a linear detection range for E2 from 1 to 200 pM, with an LOD of 1.34 pM. This LOD is 15.3 times lower than that of the L1-aptasensor, highlighting the superior sensitivity of the O5 aptamer with its five-loop structure for detecting E2. The O5-aptasensor also displayed high selectivity for E2, with no cross-reactivity with structurally similar compounds such as chloramphenicol, diethylstilbestrol, bisphenol A, progesterone, and genistein. The aptasensor successfully detected E2 in spiked artificial urine and human serum samples, within an acceptable range of recovery rate and the precision criterion of RSD value. Additionally, the precision of the O5-aptasensor, as compared to hospital analysis results for blood samples from patients, was in the range of 88.91% to 102.10%. Taken together, these results suggest that the developed O5-aptasensor offers a promising tool for hospital applications, providing a cost-effective, user-friendly, and highly sensitive system for E2 detection.

Data availability

The data supporting this article have been included as part of the ESI.†

Author contributions

We declare that we contributed significantly to the research study. Pakawat Kongpreecha also conducted experiments, collected data, and drafted the manuscript. Arnon Buntha conducted experiments and collected the data. Pattama Tongdee worked with aspects related to the SUT hospital. Pinwen Peter Chiou assisted on the discussion. Sineenat Siri, the principal investigator, designed the research, provided the reagents and instrumentation, and reviewed, discussed, and edited the manuscript.

Conflicts of interest

There are no conflicts to declare.

Acknowledgements

References

1 D. Liu, X. Chen, Y. Li, G. Sun, J. Gao, H. Nie and C. Li, *Sens. Actuators, B*, 2025, **424**, 136929.

2 T. Miyamoto and T. Shiozawa, *Gynecol. Endocrinol.*, 2019, **35**, 370–375.

3 S. S. Zahraee, N. Alvandi, M. Ghamari and N. Esfandiari, *Nano-Struct. Nano-Objects*, 2023, **34**, 100951.

4 D. J. Handelsman, E. Gibson, S. Davis, B. Golebiowski, K. A. Walters and R. Desai, *J. Endocr. Soc.*, 2020, **4**, bvaa086.

5 X. Tian, H. Song, Y. Wang, X. Tian, Y. Tang, R. Gao and C. Zhang, *Talanta*, 2020, **220**, 121367.

6 Y. Tang, Y. Hu, P. Zhou, C. Wang, H. Tao and Y. Wu, *J. Agric. Food Chem.*, 2021, **69**, 2884–2893.

7 Y. Shao, X. Qi, H. Wang, B. Tang, Y. Cheng, Z. Zhang, X. Zhang and M. Zhu, *Biosens. Bioelectron.*, 2025, **270**, 116930.

8 Z. Guo, B. Yang, W. Lu, Z. Tian and H. Hao, *Anal. Chem.*, 2024, **96**, 3655–3661.

9 W. Huang, Y. Wang, L. Wang, C. Pan and G. Shen, *Anal. Methods*, 2021, **13**, 90–98.

10 J. Wu, W. Ahmad, J. Zhang, W. Wei, J. Yu, W. Zhang, Q. Chen and Q. Ouyang, *Sens. Actuators, B*, 2023, **390**, 133999.

11 H. Jiang, Y. Liu, C. Tang, Z. Wei, M. Chen, X. Lu, J. Yang and P. Yu, *Microchem. J.*, 2024, **199**, 109968.

12 Z. Guo, B. Yang, J. Zhu, S. Lou, H. Hao and W. Lu, *Food Chem.*, 2024, **436**, 137702.

13 Y. Qin, S. Liu, S. Meng, D. Liu and T. You, *Anal. Chim. Acta.*, 2024, **1285**, 342030.

14 H. Zahraee, Z. Khoshbin, M. Ramezani, M. Alibolandi, K. Abnous and S. M. Taghdisi, *Spectrochim. Acta, Part A*, 2023, **290**, 122305.

15 H. Huang, S. Shi, X. Gao, R. Gao, Y. Zhu, X. Wu, R. Zang and T. Yao, *Biosens. Bioelectron.*, 2016, **79**, 198–204.

16 G. Zhang, T. Li, J. Zhang and A. Chen, *Sens. Actuators, B*, 2018, **273**, 1648–1653.

17 Q. Wei, P. Zhang, H. Pu and D.-W. Sun, *Food Chem.*, 2022, **373**, 131591.

18 H. Yi, Z. Yan, L. Wang, X. Zhou, R. Yan, D. Zhang, G. Shen and S. Zhou, *Microchim. Acta*, 2019, **186**, 668.

19 S. Xiao, L. Sun, J. Lu and Z. Dong, *New J. Chem.*, 2022, **46**, 16177–16182.

20 Y. Hou, X. Lu, J. Yang, C. Tang, H. Jiang, T. Cai, M. Chen, Z. Wei and P. Yu, *Anal. Methods*, 2023, **15**, 1546–1552.

21 X. Wang, J. Liu, C. Niu and J. Liu, *Adv. Agrochem*, 2023, **2**, 258–263.

22 E. P. Galay, R. Dorogin and A. Temerdashev, *Heliyon*, 2021, 7, e06046.

23 P. Kongpreecha, J. Chumpol and S. Siri, *Biotechnol. Appl. Biochem.*, 2023, **70**, 1384–1396.

24 Y. Liu, D. Zhang, J. Ding, K. Hayat, X. Yang, X. Zhan, D. Zhang, Y. Lu and P. Zhou, *Biosensors*, 2021, **11**, 133.

25 A. J. J. Amalraj, U. N. Murthy and S.-F. Wang, *ACS Appl. Nano Mater.*, 2022, **5**, 1944–1957.

26 Y. Muto, G. Hirao and T. Zako, *Anal. Sci.*, 2024, **40**, 975–979.

27 A. Cerrato, S. E. Aita, C. Cavaliere, A. Laganà, C. M. Montone, S. Piovesana, E. Taglioni and A. L. Capriotti, *Anal. Chem.*, 2024, **96**, 4639–4646.

28 X. Yao, J. Gao, K. Yan, Y. Chen and J. Zhang, *Anal. Chem.*, 2020, **92**, 8026–8030.

29 N. Wang, H. Li, Y. Tian, L. Tan, S. Cheng and J. Wang, *Microchim. Acta*, 2024, **191**, 249.

30 S. Bhogal, I. Mohiuddin, S. Kumar, A. K. Malik, K.-H. Kim and K. Kaur, *Sci. Total Environ.*, 2022, **847**, 157356.

31 H. Sha and B. Yan, *J. Colloid Interface Sci.*, 2021, **583**, 50–57.

32 S. Liu, N. Yin, Y. Zhao, B. Yan, S. Li and S. Gao, *Talanta*, 2025, **283**, 127071.

33 Y. Zhang, L. Jia, W. Wang, M. Jiang, H. Zhang and L. Niu, *Arab. J. Chem.*, 2023, **16**, 105340.

34 N. Li, C. Ren, Q. Hu, B. Wang, Z. Yang, L. Xiao and T. Guan, *Food Chem.*, 2025, **463**, 141395.

35 A. Eisold and D. Labudde, *Molecules*, 2018, **23**, 1690.

36 E. Okada, T. Coggan, T. Anumol, B. Clarke and G. Allinson, *Anal. Bioanal. Chem.*, 2019, **411**, 715–724.